



University  
of Glasgow

Warburton, R.E., Izdebski, F., Reimer, C., Leach, J., Ireland, D.G., Padgett, M. , and Buller, G.S. (2011) *Single-photon position to time multiplexing using a fiber array*. Optics Express, 19 (3). pp. 2670-2675. ISSN 1094-4087 (doi:10.1364/OE.19.002670)

<http://eprints.gla.ac.uk/59797/>

Deposited on: 7 February 2012

# Single-photon position to time multiplexing using a fiber array

Ryan E. Warburton,<sup>1,\*</sup> Frauke Izdebski,<sup>1</sup> Christian Reimer,<sup>1</sup> Jonathan Leach,<sup>2</sup>  
David G. Ireland,<sup>2</sup> Miles Padgett,<sup>2</sup> and Gerald S. Buller<sup>1</sup>

<sup>1</sup>*SUPA, School of Engineering and Physical Sciences, Heriot-Watt University, Edinburgh, EH14 4AS, UK*

<sup>2</sup>*SUPA, Department of Physics & Astronomy, University of Glasgow, Glasgow, G12 8QQ, UK*

\**r.e.warburton@hw.ac.uk*

**Abstract:** A 1 x 8 fiber array is used as the front-end of a receiver system. Each channel has a different length of fiber, resulting in each channel signal arriving at the detector at a pre-determined interval relative to a constant repetitive frequency signal. We demonstrate that these eight channels can be efficiently coupled to an individual single-photon detector such that the arrival-time of a photon in each is distinguishable from the next. Thus, we demonstrate spatial position to time information exchange, resulting in a photon-counting array using a single detector. The receiver system could be implemented in numerous applications, including time-resolved photoluminescence, low-light level spectroscopy and quantum information processing.

©2011 Optical Society of America

**OCIS codes:** (040.1240) Arrays; (270.5570) Quantum detectors.

---

## References and links

1. L. Zhang, L. Neves, J. S. Lundeen, and I. A. Walmsley, "A Characterization of the Single-photon Sensitivity of an Electron Multiplying Charge-Coupled Device," *J. Phys. B* **42**(11), 114011 (2009).
2. F. Zappa, S. Tisa, S. Cova, P. Maccagnani, D. B. Calia, R. Saletti, R. Roncella, G. Bonanno, and M. Belluso, "Single-Photon Avalanche Diode Arrays for Fast Transients and Adaptive Optics," *IEEE Trans. Instrum. Meas.* **55**(1), 365–374 (2006).
3. A. R. Altman, K. G. Köprülü, E. Corndorf, P. Kumar, and G. A. Barbosa, "Quantum imaging of nonlocal spatial correlations induced by orbital angular momentum," *Phys. Rev. Lett.* **94**(12), 123601 (2005).
4. H. Dautet, P. Deschamps, B. Dion, A. D. Macgregor, D. Macsween, R. J. McIntyre, C. Trotter, and P. P. Webb, "Photon counting techniques with silicon avalanche photodiodes," *Appl. Opt.* **32**(21), 3894–3900 (1993).
5. S. Cova, A. Longoni, and A. Andreoni, "Towards picosecond resolution with single-photon avalanche diodes," *Rev. Sci. Instrum.* **52**(3), 408–412 (1981).
6. G. S. Buller, and R. J. Collins, "Single-photon generation and detection," *Meas. Sci. Technol.* **21**(1), 012002 (2010).
7. C. E. Shannon, "A mathematical theory of communication," *Bell Syst. Tech. J.* **27**, 379 (1948).
8. Y. Hiraoka, T. Shimi, and T. Haraguchi, "Multispectral imaging fluorescence microscopy for living cells," *Cell Struct. Funct.* **27**(5), 367–374 (2002).
9. J. J. Field, R. Carriles, and J. Squier, "Photon-Counting Photobleaching Measurements and the Effect of Dispersion in Two-Photon Microscopy," Conference on Lasers and Electro-Optics/International Quantum Electronics Conference, Optical Society of America, JTuD58, (2009)
10. A. McCarthy, R. J. Collins, N. J. Krichel, V. Fernández, A. M. Wallace, and G. S. Buller, "Long-range time-of-flight scanning sensor based on high-speed time-correlated single-photon counting," *Appl. Opt.* **48**(32), 6241–6251 (2009).
11. M. N. O'Sullivan-Hale, I. A. Khan, R. W. Boyd, and J. C. Howell, "Pixel entanglement: experimental realization of optically entangled d=3 and d=6 qudits," *Phys. Rev. Lett.* **94**(22), 220501 (2005).

---

## 1. Introduction

There is an increasing requirement to measure low-light levels with picosecond resolution simultaneously at multiple spatial positions. Single-photon cameras are commercially available [1] and are typically based on electron-multiplying CCDs (EMCCDs). These cameras demonstrate single-photon sensitivity. Unfortunately, whilst they offer position sensitivity, they lack the nanosecond or picosecond temporal resolution necessary in a number

of emerging applications. Single-photon avalanche diode (SPAD) detector arrays [2] offer the possibility of simultaneous single-photon measurements at multiple positions whilst maintaining picosecond resolution timing signatures. However this approach introduces further challenges such as crosstalk, fill-factor (which may typically be lower than 5%), fast data multiplexing and potential non-uniformities in detector performance. Using many individual detectors and acquisition hardware is also a solution, however this is a cumbersome and expensive approach.

Instead of using a detector array, an individual detector, which is scanned across the desired positions, can be used [3]. While this alternative is more cost effective, the scanning process may result in position errors during movement, and does not permit the simultaneous acquisition of data from multiple spatial positions, leading to greatly increased acquisition times in these photon-starved measurements.

The method presented in this paper is an alternative to these approaches. We use a fiber array with a fiber combiner, as this combines the ability to measure multiple spatial positions simultaneously with the cost efficiency and performance of using only one optimized detector. Not only is the temporal information recorded and correlated to spatial position, it is also possible - most relevant in applications such as time-resolved photoluminescence (TRPL) - to observe differences in temporal response from different areas of the sample under test.

The fiber array is housed in a V-groove fabricated from silicon where the V-groove pitch is 127  $\mu\text{m}$ . Eight grooves are anisotropically etched into the silicon, each V-groove holds one fiber with a core diameter of 50  $\mu\text{m}$  and a cladding diameter of 125  $\mu\text{m}$ . The fibers are all evenly stepped in length, resulting in different pre-determined signal arrival intervals at the detector. The eight fibers housed in the V-groove are FC/PC connectorized on the exit ends. These eight fibers are coupled into a single detector using a fiber combiner which efficiently combines eight input fibers to a single output fiber. The core diameter of the input fibres was chosen to be 50  $\mu\text{m}$  to match the core diameter of the V-groove fibers and therefore enable efficient fiber to fiber coupling from the fiber array. In practice, the coupling loss between array and combiner fibers is estimated to be  $\sim 0.2$  dB per fiber. In the combiner fabrication process, the input fibers are first stretched and tapered, then fusion spliced onto the output fiber, which has a larger core diameter of 105  $\mu\text{m}$ . In this experiment, the output fiber is then coupled into a single-photon detector. The average transmittance of the combiner is  $\sim 70\%$  across all 8 channels, with a maximum of 78% in channel 2 and a minimum of 65% in channel 8.

## 2. Experimental setup

To characterize the receiver, the setup in Fig. 1 was used. The characterization setup consists of a pulsed laser diode emitting at a wavelength of 686 nm, the measurements were then repeated with a 850 nm wavelength laser to ascertain any spectrally dependent loss. The laser was coupled into a 5  $\mu\text{m}$  diameter fiber to circularize the optical beam, and an optical fiber power meter is used to monitor the laser power stability. The collimated laser beam was attenuated by neutral density filters such that much less than one photon per pulse was entering any individual fibre. The beam was aligned to fully, and equally, illuminate all fibers of the V-groove array. A transmission slit was added to characterize the channel capacity as shown later. The V-groove fibers were connected to the combiner and the single output fiber of the combiner was attached to the SPAD under test - either a thick pn-junction SPAD [4] (Perkin Elmer, model number: SPCM-CD2882) or a thin pn-junction SPAD [5] (MPD, model number: PDF series with 62.5  $\mu\text{m}$  graded index fiber). The repetitive signal that was used to drive the laser was also used to start the timing electronics of the photon-counting hardware. The SPAD signal was used as the stop signal such that many measurements of single-photon events were collected to produce the photon-counting timing histograms shown in Figs. 2 and 3.

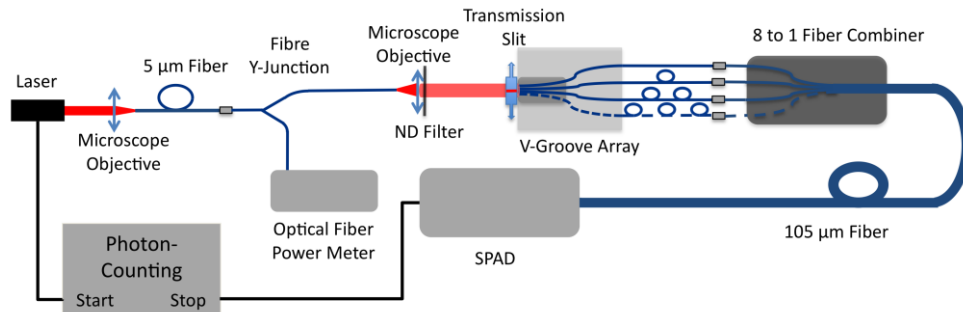


Fig. 1. Characterization setup (for clarity, only four V-groove fibers are shown).

### 3. Experimental results

In order to establish the maximum throughput of the system, each fiber from the array was connected directly to a thick junction SPAD of known detection efficiency. The combiner was then added to the setup to fully characterize the system. The results are presented in Table 1 in terms of overall single-photon detection efficiency (SPDE) and detector jitter.

**Table 1. Comparison of the single-photon detection efficiency and the jitter of selected SPADs**

Detector	SPDE [%]	FWHM [ps]
Thick junction SPAD	41.7	687 ( $\sigma = 22$ )
Thin junction SPAD	5.5	135 ( $\sigma = 3$ )

Characterization of the different detector setups shows that the thick junction SPAD has a high SPDE but also a large timing jitter due to the thick absorbing region of the detector [6]. Although the eight peaks are clearly distinguishable, the timing jitter causes an overlap between two adjacent peaks as shown in the dotted trace in Fig. 2. The tail of the previous channel adds counts to the next channel.

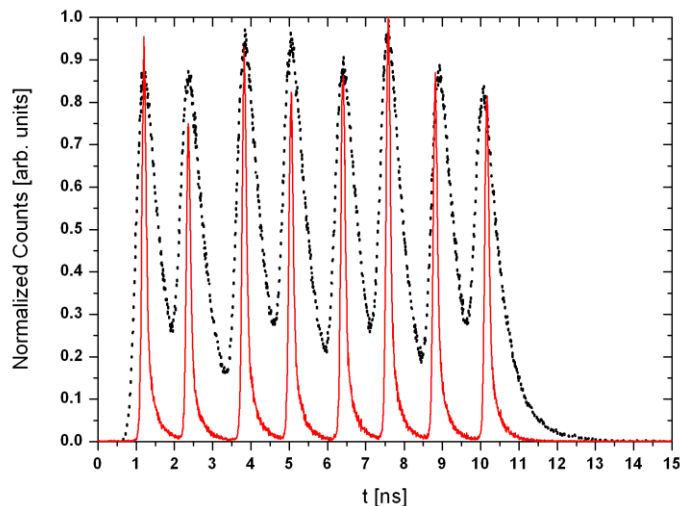


Fig. 2. Histogram for thin-junction (solid line) and thick-junction (dotted line) SPAD showing experimental data when the fiber combiner is directly connected to the respective SPAD.

The thin junction SPAD results indicate a low jitter without significant overlap between two adjacent peaks (solid line trace in Fig. 2). When the fiber combiner is directly connected to the thin junction SPAD the timing jitter is 135 ps. One has to mention that the thin junction

detector with an active area diameter of 50  $\mu\text{m}$  is coupled to a fiber with a core diameter of 62.5  $\mu\text{m}$  so that it is not possible to measure the SPDE and timing jitter with the larger 105  $\mu\text{m}$  diameter fiber because some higher order modes are suppressed during the coupling process.

The temporal separation between peaks is determined by the selection of the optical fiber length before the combiner stage. The spacing used in these measurements was aimed at measuring 8 different positions in a 10 ns window for compatibility with a 100 MHz repetition rate source. Longer fibres will further improve the temporal separation at the expense of overall data rate. Using a detector with lower jitter would enable decreased temporal separation of channels. This could be exploited in two ways: either more channels within a 10 ns period, for example, or the same number of channels but a higher repetition frequency.

To show the capability of the fiber array to convert positional information into time information, we placed a transmission slit directly in front of each of the V-groove fibers as shown in the lower part of Fig. 3. The width of the slit was less than the separation between the two fibers cores such that at any one position, only one of the fibres of the V-groove would collect light. The timing signature for each of the 8 positions was recorded using the thin junction SPAD, and these traces are plotted in Fig. 3. The peak position in each of these plots corresponds to a unique time thus identifying the different positions of the transmission slit.

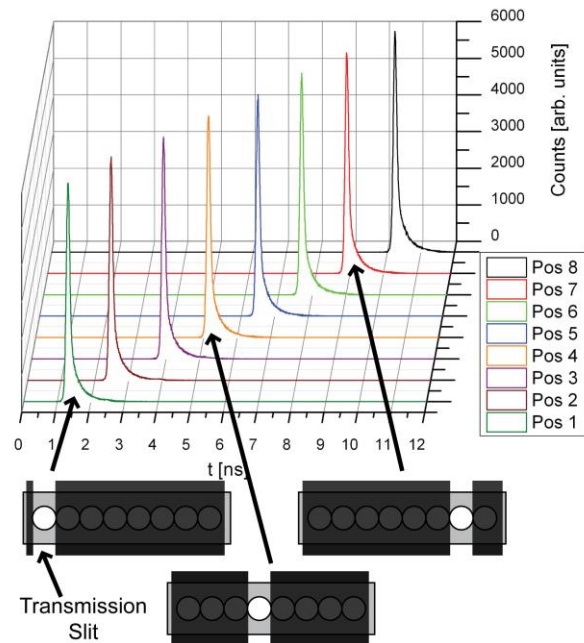


Fig. 3. Position to time measurements using the fiber array and the thin junction SPAD. The lower part of the Figure represents the positioning of the transmission slit, demonstrating its position relative to that of the peak in the photon-counting histogram. The slight variations in peak height are due to the nominal differences in efficiency of each channel within the combiner.

These results can be analysed to quantify the channel capacity or number of effective channels that the combination of the fiber array and detector can measure. This is an important number to quantify when considering such a device for single-photon communication systems. This is analogous to characterising the performance of a polarizing beam splitter used to sort input polarisation states.

For the channel capacity calculation, the spatial positions of the slit are the input states,  $\{a_1, a_2, \dots, a_8\}$ . The receiver states,  $\{b_1, b_2, \dots, b_8\}$ , are specific time windows in the recorded histogram, the separation between the states set by the optical delay introduced by the additional optical fibre. The probability of recording a state  $P(b_i)$  is calculated by summing the counts in the corresponding time window and dividing by the sum of all the counts in all windows. From information theory [7], the channel capacity of the system is then,

$$C = H(a:b) = H(a) - H(a|b) \quad (1)$$

where in our case,

$$H(a) = -\sum_{a_i} P(a_i) \log_2 P(a_i) \quad (2)$$

is the entropy of the source, and

$$H(a|b) = -\sum_{a_i} \sum_{b_i} P(a_i, b_i) \log_2 P(a_i | b_i) \quad (3)$$

is the conditional entropy of transmitted signal  $a$  given received signal  $b$ .

Given that the maximum possible number of modes for the V-groove fiber array is 8, if used in a single-photon communication system, this would correspond to 3bits/photon. In practice, the finite width of the detection signal and the background counts arising from the detector result in a reduced channel capacity and number of modes. With no additional windowing of the data, the channel capacity of the fibre array and the thick junction detector was found to be  $C = 2.32$  bits/photon with 4.99 effective modes, the thin junction SPAD described above was found to be  $C = 2.63$  bits/photon corresponding to 6.17 effective modes as shown in Table 2. This can be increased through selective binning of the expense of the overall data rate of the device. For example, by selecting the bins for the receiver state to be the width  $(1/e)$  of a Gaussian fitted to the signal we can increase the effective mode channel capacity to  $C = 2.58$  bits/photon with 6.00 modes and  $C = 2.93$  bits/photon with 7.60 modes for the thick and thin junction SPADs respectively. The decrease in the transmission rate that this windowing results in is around 42% for the thick junction SPAD and 47% for the thin junction SPAD.

**Table 2. Comparison of the number of modes and bits per photon for different detectors and binned data**

SPAD	Bit/photon	No. modes	Bit/photon (binned)	No. modes (binned)	Transmission rate (binned)
Thick Junction	2.32	4.99	2.58	6.00	58%
Thin Junction	2.63	6.17	2.93	7.60	53%

Applications that require low light level detection and multiple measurement points at the same time will benefit from the fiber array approach. Applications include TRPL, fluorescence lifetime imaging (FLIM), and spectroscopy of faint optical sources, e.g. single-photon sources. One example is the multi-spectral time-resolved fluorescence where multiple wavelengths are measured simultaneously for rapid data acquisition [8] and to avoid effects such as photobleaching [9]. Other applications like photon-counting time-of-flight depth imaging [10] and quantum imaging will benefit from the increased data rate of the receiver system and the possibility to obtain full-field images.

One possible application of the multi-channel receiver is in the field of quantum imaging where coincidence measurements are made on signal and idler photons produced by spontaneous parametric downconversion (SPDC). If each downconversion arm possesses an identical fiber array, combiner and one detector, measurements can be performed to assess the strength of position correlations. So far multichannel measurements have been realised with

the use of fiber arrays, where each fiber is pigtailed to an individual detector [11] and thus adding complexity to the receiver system as each detector varies in efficiency, timing jitter and dark current. With the aid of the fiber array it is possible to obtain coincidence measurements without the use of several detectors in each arm and without scanning with a single detector, where photons, and therefore coincidences, will be lost during the scan. The fiber array receiver system is a cost effective and user-friendly alternative for existing receiver systems.

#### **4. Conclusions**

Position to time multiplexing using a fiber array has been demonstrated in a single-photon detection scheme. This approach offers the opportunity to measure multiple positions at low light levels simultaneously without the need for scanning and with the ease of using only an individual optimized single-photon detector. While dealing with low light levels, care has to be taken that only a minimum of light is lost. The described receiver system efficiently couples the eight input fibres to a single output fibre and therefore fulfils this requirement. The possibility to measure different positions simultaneously leads to an increased data acquisition rate. Therefore, applications where the time range for taking data is limited will benefit from this receiver system. Applications include FLIM, ranging and quantum imaging.

#### **Acknowledgements**

Both Heriot-Watt University and the University of Glasgow would like to acknowledge funding for this work from the UK Engineering and Physical Research Council (grant numbers: G01163X and G011656 respectively).